Chapter 2

Interaction among offset cracks in orthotropic medium under thermo-mechanical loadings

2.1 Introduction

2.1.1 Background

Materials are often subject to various stresses during their service life. Cracks, which are common in materials, can grow when they reach a critical size, potentially leading to failure. The presence of a steady-state heat flux can exacerbate this issue by inducing thermal stresses around the cracks. When these stresses surpass the material's resistance, the risk of catastrophic failure increases. The concept of stress intensity is crucial in fracture mechanics as it quantifies stress distribution around a crack tip [48, 49, 50]. It is a measure of a material's fracture toughness. The

SIF (K) characterizes the behaviour of stress near the crack tip, which exhibits a square-root singularity, necessitating detailed stress analysis in the vicinity of the crack [51, 52]. Fiber-reinforced composite (FRC) materials have become popular due to their advantageous properties, such as high stiffness, low weight, and considerable strength. These materials are used in various applications, including aircraft, submarines, civil infrastructure, and robotics [53]. The unidirectional alignment of fibers within the matrix grants these materials orthotropic properties. However, the matrix, being softer and weaker compared to the fibers, is more prone to deformation [54]. The interplay between thermal stresses and material resistance is a critical aspect of material design, especially in the context of FRC materials. Understanding and mitigating the effects of these stresses can prevent structural failures and extend the lifespan of the materials.

2.1.2 Literature survey and Research gaps

The investigation of stress singularities in two-dimensional problems, such as those studied by Sih [55] using complex variable methods, marks a significant milestone in crack kinematics analysis. Sih's work primarily addressed the thermal stress singularities at the crack tip under steady-state temperature distributions. Subsequent studies, including those by Ang and Williams, [56], employed integral equation methods to analyze stress and displacement fields in orthotropic planes with finite cracks. Pioneers like Stroh [57], Tsai [54], and Florence and Goodier [58] have focused on stresses around single cracks, solving linear thermo-elasticity problems using Fourier, Hankel, and Hilbert transforms, along with multiple integrals. These integral transform techniques reformulate the equations of motion into integral equations whose solutions yield the SIFs. For instance, the work in [59] explored an ovoidal-shaped crack, with ellipses and circles as special cases, using conformal transformations

to derive closed-form solutions. Chang [60] examined an orthotropic solid with two collinear cracks under thermo-mechanical loading, applying the Fourier transformation to derive triple integral equations that describe the thermoelastic fields, including strain energy density, stress intensity, temperature jumps, and elastic displacements across the cracks. Chen and Zheng [61] discovered that extreme stress singularities could arise when the distance between two collinear cracks diminishes by converting the mixed boundary value problem into pairs of integral equations solved via finite Hilbert transform. This phenomenon has been corroborated by numerous studies that solve coupled Cauchy-type singular integral equations to determine thermal stress solutions [62]. The influence of crack orientations on various parameters was examined by [63], which analyzed two arbitrarily oriented cracks in an elastic solid. Mauge and Kachanov [64] further discussed the impact of geometry and parameters on the SIFs of interacting cracks in an orthotropic plane. Research by Faal and Fariborz [65] derived stress fields for mode I and mode II cracks under in-plane loads, while Binienda and Arnold [66] investigated a multi-cracked plate's behavior by calculating the SIFs and strain energy release rates. These studies predominantly assume isothermal conditions, with the exception of Sekine [67], who addressed the interaction of two cracks in an isotropic plane. Choi [9] explored the thermoelastic problem of offset cracks in an FRC medium. However, the study of interactions between three cracks such that there are two cracks offset to a central crack in an orthotropic plane under thermo-mechanical loadings remains unexplored, presenting a novel avenue for research.

2.1.3 Chapter organisation

This chapter delves into the thermoelastic challenges associated with two-dimensional insulated cracks. The geometry of the considered problem with the basic problem

formulation and the governing equations, including the constitutive relations, equilibrium and compatibility conditions, are mentioned in Section 2.2; specifically, it examines a scenario where two offset cracks are aligned parallel to a central crack within an orthotropic plane, all under the influence of thermo-mechanical loadings. The Section 2.3 includes the application of the Fourier integral transformation technique to the heat conduction equations, and the displacement field equations facilitate the derivation of dual Cauchy-type singular integral equations, which are specified in the Section 2.4. The numerical solution is obtained by using the expansion collocation technique with a Chebyshev polynomial of the first kind. The orthogonality conditions and weight functions for the Chebyshev polynomial are detailed in Section 2.5. The SIFs at the tips of the cracks are meticulously determined, computed, and discussed in Section 2.6. Here, an exemplar FRC material is utilized to calculate the numerical values of these SIFs. The study elucidates the effects of varying applied loadings on the SIFs through illustrative depictions. It is observed that an adequate separation between the cracks can significantly mitigate their mutual influence. Finally, a conclusion Section 2.7 is included to summarize the contents of the chapter.

2.2 Problem Formulation

Consider an infinite orthotropic plane subjected to a uniform heat flux of magnitude q_0 and mechanical loading with a stress component normal to the crack surface. The unidirectional fibre structure ensures orthotropy in the horizontal direction that is aligned with the cracks. For the sake of clarity in the mathematical calculations and interpretations, we have categorized the plane into two half-planes (labelled 2, 3) and a layer of width h (labelled 1) between them. Figure 2.1 depicts the geometry

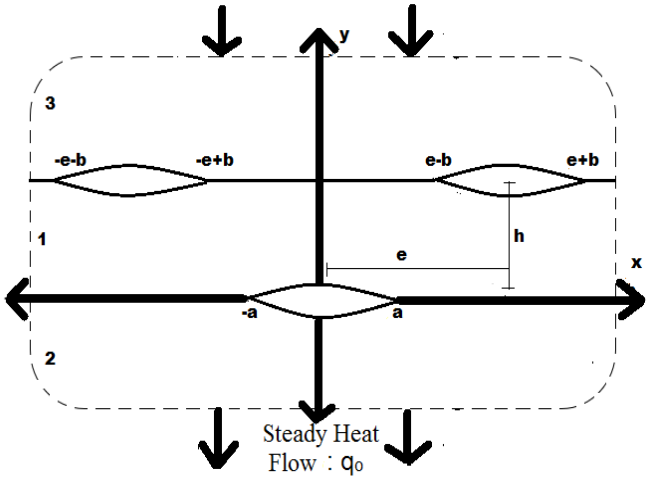

FIGURE 2.1: An infinite orthotropic plane with uniform heat flow of magnitude q_o along the y-direction.

of three thermally insulated cracks present in the orthotropic plane. A rectangular coordinate system with (x, y) is considered a Cartesian coordinate. The central crack located at $(-a, a)$ aligns with the x-axis at an offset parallel distance from the two collinear cracks located on the upper edge, h at $(e-b, e+b)$ and $(-e-b, -e+b)$, respectively. The symmetry of the problem allows us to carry the calculation only for the $x \geq 0$ plane.

2.2.1 Temperature Field

Governing equations and constitutive relations The heat (thermal) flux equation is given, for example, by Milton [31] and Aboudi et al.[68]

$$\mathbf{Q(x)} = -\mathbf{K(x)} \cdot \mathbf{E(x)} \quad \text{with the differential constraints as} \quad \boldsymbol{\nabla} \cdot \mathbf{Q} = 0, \ \boldsymbol{\nabla} \times \mathbf{E} = \mathbf{0}, \tag{2.1}$$

where $\mathbf{Q}$ denotes heat flux vector, $\mathbf{E} = \boldsymbol{\nabla} T$ represents the temperature gradient with the absolute temperature T, $\mathbf{K}$ is the thermal conductivity tensor, $\boldsymbol{\nabla}$ is the nabla

(Hamilton) operator and $\cdot$ is the scalar (dot) product. The constraints mean that there is zero heat flux through an enclosing surface (no sources or sinks), and the temperature gradient is irrotational. Hence, Fourier's law of thermal conduction is stated as

$$\vec{q} = -K\nabla T. \tag{2.2}$$

where q_x and q_y, heat flux components of vector $\mathbf{Q}$ in x and y directions, respectively are given by

$$q_x = -k_x\, T_{,x}\ , \qquad q_y = -k_y\, T_{,y}. \tag{2.3}$$

From the differential constraints, the heat conduction equation becomes

$$q_{x,x} + q_{y,y} = 0. \tag{2.4}$$

The undisturbed temperature field is given by $\frac{q_0}{k_y}y$, and the original temperature disturbed by cracks is $T(x,y)$ [54]. Hence, the complete temperature field is conveniently represented as $\frac{q_o}{k_y}y + T(x,y)$. Using the Energy-Balance equation and considering the net energy generation as zero, under the steady-state condition, from the differential constraints given in equation (2.1), it is evident that

$$k_x^{(i)}\, T_{,xx}^{(i)} + k_y^{(i)}\, T_{,yy}^{(i)} = 0, \tag{2.5}$$

where $k^{(i)} = \sqrt{k_x^{(i)}/k_y^{(i)}}$, is the ratio of thermal conductivity coefficients in y and x directions, respectively and throughout the thesis, the superscript (i) denotes the subsequent considered plane. Applying the Fourier cosine transformation given in the expression (1.28a) over the variable x, the equation (2.5) reduces to the following

equation in the transformed domain s as

$$-k^{(i)2}s^2\overline{T^{(i)}}(s,y)+\overline{T^{(i)}_{,yy}}(s,y)=0. \tag{2.6}$$

Over the condition that the field quantity and its first order derivative vanishes at $x=\pm\infty$, the equation (2.6) yields the general solution of steady-state temperature field $T(x,y)$ in the following forms [9]

$$\overline{T}^{(1)}(s,y)=\left(A_{11}(s)e^{sky}+A_{12}(s)e^{-sky}\right), \tag{2.7a}$$

$$\overline{T}^{(2)}(s,y)=A_{21}(s)e^{sky}, \tag{2.7b}$$

$$\overline{T}^{(3)}(s,y)=A_{31}(s)e^{-sky}, \tag{2.7c}$$

where $A_{ij}(s)$'s are the unknown functions. The solution procedure involves determining the disturbed temperature field under some boundary conditions. Mathematically, the boundary and continuity conditions of temperature for the considered problem are changed to

$$T^{(1)}_{,y}(x,h)=T^{(3)}_{,y}(x,h),\quad 0<x<\infty, \tag{2.8a}$$

$$T^{(1)}_{,y}(x,0)=T^{(2)}_{,y}(x,0),\quad 0<x<\infty, \tag{2.8b}$$

$$T^{(1)}_{,y}(x,h)=\frac{-q_o}{k_y},\quad e-b<x<e+b, \tag{2.8c}$$

$$T^{(1)}_{,y}(x,0)=\frac{-q_o}{k_y},\quad 0<x<a, \tag{2.8d}$$

$$T^{(j)}(x,y)=0,\ j=2,3,\quad \sqrt{x^2+y^2}\to\infty, \tag{2.8e}$$

$$T^{(1)}(x,h)=T^{(3)}(x,h),\quad x<e-b, x>e+b, \tag{2.8f}$$

$$T^{(1)}(x,0)=T^{(2)}(x,0),\quad x>a. \tag{2.8g}$$

Continuity conditions (2.8a) and (2.8b) are based on the statement that heat conduction at the surface of planes 1, 2 and 3 are the same. Here, assuming that the heat flux q_o is known, the boundary conditions (2.8c) and (2.8d) specify the values that the solution term will take along the boundary of the domain. Condition (2.8e) is the regularity condition for the temperature field.

2.2.2 Displacements and Thermal Stresses

In the theory of linear elasticity for a body at equilibrium and in the absence of body forces, the tensile and shear stress components are related to displacement gradient vector through the following relations [69, 70]

$$\boldsymbol{\sigma}(\mathbf{x}) = \mathbf{C}(\mathbf{x}) \cdot \boldsymbol{\varepsilon}(\mathbf{x}) \quad \text{with the differential constraints as } \boldsymbol{\nabla} \cdot \boldsymbol{\sigma} = 0,\ \boldsymbol{\nabla} \times \boldsymbol{\varepsilon} = 0, \tag{2.9}$$

where $\boldsymbol{\sigma}$ denotes stress field, $\boldsymbol{\varepsilon} = -[\nabla \mathbf{u} + \nabla \mathbf{u}^{\mathrm{T}}]/2$ is the strain field (T means transposed), $\mathbf{C}$ is the elastic stiffness tensor that connects the two fields through a constitutive relation and $\mathbf{u}$ is the displacement vector. The constraints are the equilibrium equation (without body forces) and the compatibility condition of the strain tensor.

Let $u(x, y)$ and $v(x, y)$ denote the non-vanishing displacement functions in x and y direction, respectively. The stresses induced due to thermo-mechanical loadings follow the constitutive equations of thermo-elasticity. So, in the state of plane stress,

Duhamel-Neumann equations for shear and normal components of stresses are obtained from Hooke's law [69] as

$$\sigma_{xx} = C_{11}u_{,x} + C_{12}v_{,y} - \beta_1 T, \tag{2.10}$$

$$\sigma_{yy} = C_{12}u_{,x} + C_{22}v_{,y} - \beta_2 T, \tag{2.11}$$

$$\tau_{xy} = C_{66}(u_{,y} + v_{,x}), \tag{2.12}$$

Using the relations obtained from the differential constraints, we get

$$\sigma_{xx,x} + \tau_{xy,y} = 0, \tag{2.13a}$$

$$\tau_{xy,x} + \sigma_{yy,y} = 0, \tag{2.13b}$$

with the stress expressions given in equations (2.10)-(2.12), the Navier-Cauchy equations of equilibrium are obtained as

$$C_{11}^{(i)}\ u_{,xx}^{(i)} + C_{66}^{(i)}\ u_{,yy}^{(i)} + L^{(i)}\ v_{,xy}^{(i)} = \beta_1^{(i)}\ T_{,x}^{(i)}, \tag{2.14a}$$

$$C_{66}^{(i)}\ v_{,xx}^{(i)} + C_{22}^{(i)}\ v_{,yy}^{(i)} + L^{(i)}\ u_{,xy}^{(i)} = \beta_2^{(i)}\ T_{,y}^{(i)}\ , \tag{2.14b}$$

where $L^{(i)} = (C_{12}^{(i)} + C_{66}^{(i)})$, $C_{11} = \frac{E_{xx}}{1-\nu_{yx}\nu_{xy}}$, $C_{22} = \frac{E_{yy}}{1-\nu_{yx}\nu_{xy}}$, $C_{12} = \frac{E_{yy}\nu_{xy}}{1-\nu_{yx}\nu_{xy}} = \frac{E_{xx}\nu_{yx}}{1-\nu_{yx}\nu_{xy}}$, $C_{66} = G_{xy}$. with E_{xx}, E_{yy} are Young's moduli, G_{xy} is shear modulus, ν_{xy}, ν_{yx} are Poisson's ratios. The thermal moduli are written in terms of material properties and thermal expansion coefficients α_{xx}, α_{yy} as

$$\begin{bmatrix} \beta_1 \\ \beta_2 \end{bmatrix} = \begin{bmatrix} C_{11} & C_{12} \\ C_{12} & C_{22} \end{bmatrix} \begin{bmatrix} \alpha_{xx} \\ \alpha_{yy} \end{bmatrix}.$$

Applying Fourier sine and cosine transformations on u and v in equations, we get

$$s^2\ C_{11}^{(i)}\ \overline{u}^{(i)} - C_{66}^{(i)}\ \overline{u}_{,yy}^{(i)} + s^2\ (C_{66}^{(i)} + C_{12}^{(i)})\ \overline{v}_{,y}^{(i)} = s\ \beta_1^{(i)}\overline{T^{(i)}}, \tag{2.15a}$$

$$-(C_{66}^{(i)} + C_{12}^{(i)})\ \overline{u}_{,y}^{(i)} + s^2\ C_{66}^{(i)}\ \overline{v}^{(i)} - C_{22}^{(i)}\ \overline{v}_{,yy}^{(i)} = \beta_2^{(i)}\ \overline{T_{,y}^{(i)}}. \tag{2.15b}$$

The general solutions of (2.15a) and (2.15b) are obtained in terms of Fourier integral sine and cosine functions as

$$\begin{aligned}\overline{u}^{(1)}(s,y) = \big(&B_{11}(s)e^{s\lambda_1 y} + B_{12}(s)e^{s\lambda_2 y} + B_{13}(s)e^{-s\lambda_1 y} + B_{14}(s)e^{-s\lambda_2 y} \\ &+\frac{\eta_1}{s}A_{11}(s)e^{sky} + \frac{\eta_1}{s}A_{12}(s)e^{-sky}\Big),\end{aligned} \tag{2.16a}$$

$$\overline{u}^{(2)}(s,y) = \left(B_{21}(s)e^{s\lambda_1 y} + B_{22}(s)e^{s\lambda_2 y} + \frac{\eta_1}{s}A_{21}(s)e^{sky}\right), \tag{2.16b}$$

$$\overline{u}^{(3)}(s,y) = \left(B_{31}(s)e^{-s\lambda_1 y} + B_{32}(s)e^{-s\lambda_2 y} + \frac{\eta_1}{s}A_{31}(s)e^{-sky}\right), \tag{2.16c}$$

$$\begin{aligned}\hat{v}^{(1)}(s,y) = \big(&B_{11}(s)\gamma_1 e^{s\lambda_1 y} + B_{12}(s)\gamma_2 e^{s\lambda_2 y} - B_{13}(s)\gamma_1 e^{-s\lambda_1 y} \\ &-B_{14}(s)\gamma_2 e^{-s\lambda_2 y} - \frac{\eta_2}{s}A_{11}(s)e^{sky} + \frac{\eta_2}{s}A_{12}(s)e^{-sky}\Big),\end{aligned} \tag{2.16d}$$

$$\hat{v}^{(2)}(s,y) = \left(B_{21}(s)\gamma_1 e^{s\lambda_1 y} + B_{22}(s)\gamma_2 e^{s\lambda_2 y} - \frac{\eta_2}{s}A_{21}(s)e^{sky}\right), \tag{2.16e}$$

$$\hat{v}^{(3)}(s,y) = \left(B_{31}(s)\gamma_1 e^{-s\lambda_1 y} + B_{32}(s)\gamma_2 e^{-s\lambda_2 y} - \frac{\eta_2}{s}A_{31}(s)e^{-sky}\right), \tag{2.16f}$$

where $B_{jk}(s)$'s are unknowns given in the Appendix A. λ_j are the roots (Re $\lambda_j > 0$) of the equation

$$C_{22}C_{66}\lambda^4 + (C_{12}^2 + 2C_{12}C_{66} - C_{11}C_{22})\lambda^2 + C_{11}C_{66} = 0. \tag{2.17}$$

Mathematical manipulations allow us to consider two distinct values for λ, which are stated in the Appendix A. Depending on it the corresponding $\gamma_j, j = 1, 2$ are

given for each eigenvalue as

$$\gamma_j = \frac{C_{11} - C_{66}\lambda_j^2}{(C_{22} + C_{66})\lambda_j}, \quad j = 1, 2, \tag{2.18}$$

with the thermo-elastic constants $\eta_j, j = 1, 2$ defined by

$$\eta_1 = \frac{(\beta_2(C_{12} + C_{66}) - \beta_1 C_{22})k^2 + \beta_1 C_{66}}{C_{22}C_{66}k^4 + (C_{12}^2 + 2C_{12}C_{66} - C_{11}C_{22})k^2 + C_{11}C_{66}}, \tag{2.19a}$$

$$\eta_2 = \frac{\beta_2 C_{66}k^3 + (\beta_1(C_{12} + C_{66}) - \beta_2 C_{11})k}{C_{22}C_{66}k^4 + (C_{12}^2 + 2C_{12}C_{66} - C_{11}C_{22})k^2 + C_{11}C_{66}}. \tag{2.19b}$$

The thermal stresses and displacements are then solved under the boundary conditions using inverse Fourier transformation. The normal and shear traction components satisfy the set of mixed mechanical boundary and continuity conditions given by

$$u^{(j)}(x, y) = v^{(j)}(x, y) = 0, j = 2, 3; \qquad \sqrt{x^2 + y^2} \to \infty, \tag{2.20a}$$

$$u^{(3)}(x, h) = u^{(1)}(x, h), \quad v^{(3)}(x, h) = v^{(1)}(x, h), \quad x < e - b, x > e + b, \tag{2.20b}$$

$$u^{(2)}(x, 0) = u^{(1)}(x, 0), \quad v^{(2)}(x, 0) = v^{(1)}(x, 0), \quad x > a. \tag{2.20c}$$

$$\sigma_{yy}^{(3)}(x, h) = \sigma_{yy}^{(1)}(x, h),\ \tau_{xy}^{(3)}(x, h) = \tau_{xy}^{(1)}(x, h), \quad 0 < x < \infty, \tag{2.20d}$$

$$\sigma_{yy}^{(1)}(x, 0) = \sigma_{yy}^{(2)}(x, 0)\ ,\ \tau_{xy}^{(1)}(x, 0) = \tau_{xy}^{(2)}(x, 0), \quad 0 < x < \infty, \tag{2.20e}$$

$$\sigma_{yy}^{(1)}(x, h) = l_1, \qquad \tau_{xy}^{(1)}(x, h) = 0, \qquad e - b < x < e + b, \tag{2.20f}$$

$$\sigma_{yy}^{(1)}(x, 0) = l_2, \qquad \tau_{xy}^{(1)}(x, 0) = 0, \qquad 0 < x < a. \tag{2.20g}$$

2.3 Solution Procedure

Proceeding by introducing the auxiliary functions for both the heat conduction problem and thermal stresses by applying conditions (2.8f)-(2.8g) as

$$f_1(x) = T^{(3)}_{,x}(x,h) - T^{(1)}_{,x}(x,h), \quad 0 < x < \infty, \tag{2.21a}$$

$$f_2(x) = T^{(1)}_{,x}(x,0) - T^{(2)}_{,x}(x,0), \quad 0 < x < \infty. \tag{2.21b}$$

Under the boundary and continuity conditions of the temperature field outside the cracks, the expressions (2.21a)-(2.21b) fulfill the following conditions

$$f_1(x) = 0, \quad x < e-b, \; x > e+b, \tag{2.22a}$$

$$f_2(x) = 0, \quad x > a, \tag{2.22b}$$

$$\int_{e-b}^{e+b} f_1(x)dx = 0, \quad \int_0^a f_2(x)dx = 0. \tag{2.22c}$$

Incorporating the technique of inverse Fourier transformation along with the equations (2.8a), (2.8b) and some algebraic calculations on the equations, the unknowns A_{ij}'s given in (2.7a)-(2.7c) are obtained in form of auxiliary functions $f_i, i = 1, 2$. The equations (2.7a)-(2.7c) become

$$T^{(1)}(x,y) = \frac{1}{\pi}\Bigg(\int_0^\infty \frac{1}{s} \int_{e-b}^{e+b} f_1(r)\sin(sr)\cos(sx)dre^{sk(y-h)}ds - \int_0^\infty \frac{1}{s}\int_0^a f_2(r)\sin(sr)\cos(sx)dre^{-sky}ds\Bigg), \tag{2.23a}$$

$$T^{(2)}(x,y) = \frac{1}{\pi}\Bigg(\int_0^\infty \frac{1}{s} \int_{e-b}^{e+b} f_1(r)\sin(sr)\cos(sx)dre^{sk(y-h)}ds - \int_0^\infty \frac{1}{s}\int_0^a f_2(r)\sin(sr)\cos(sx)dre^{sky}ds\Bigg), \tag{2.23b}$$

$$T^{(3)}(x,y) = \frac{1}{\pi}\Bigg(\int_0^\infty \frac{1}{s} \int_{e-b}^{e+b} f_1(r)\sin(sr)\cos(sx)dre^{-sk(y-h)}ds -$$

$$\int_0^{\infty} \frac{1}{s} \int_0^{a} f_2(r) \sin(sr) \cos(sx) dr e^{-sky} ds \Big). \tag{2.23c}$$

Further, by some mathematical interpretations on equations (2.8a), (2.8b) and (2.21a), (2.21b), the equations (2.8c), (2.8d) are simplified as

$$\int_{e-b}^{e+b} L_1(x,r) f_1(r) dr + \int_0^{a} L_2(x,r) f_2(r) dr = -\frac{\pi q_o}{\sqrt{k_x k_y}}, \tag{2.24a}$$

$$\int_{e-b}^{e+b} L_2(x,r) f_1(r) dr + \int_0^{a} L_1(x,r) f_2(r) dr = -\frac{\pi q_o}{\sqrt{k_x k_y}}, \tag{2.24b}$$

where $L_{ij}(x,r),\ i,j = 1,2$ are the kernels with values

$$L_1(x,r) = \int_0^{\infty} \sin(sr) \cos(sx) ds, \tag{2.25a}$$

$$L_2(x,r) = \int_0^{\infty} e^{-skh} \sin(sr) \cos(sx) ds. \tag{2.25b}$$

To reach the desired goal, we need the following primitive trigonometric and integral identities [71]

$$\int_0^{\infty} e^{-sy} \sin s(r-x) ds = \frac{(r-x)}{y^2 + (r-x)^2}, \qquad y > 0, \tag{2.26a}$$

$$\int_0^{\infty} e^{-sy} \cos s(r-x) ds = \frac{y}{y^2 + (r-x)^2}, \qquad y > 0, \tag{2.26b}$$

$$\int_0^{\infty} \frac{1}{s} e^{-sy} \sin s(r-x) ds = \tan^{-1} \frac{(r-x)}{y}, \qquad y > 0. \tag{2.26c}$$

In order to proceed with the displacement functions, we replace the equations in (2.20a)-(2.20c) as

$$g_1(x) = v^{(3)}_{,x}(x,h) - v^{(1)}_{,x}(x,h), \quad 0 < x < \infty, \tag{2.27a}$$

$$g_2(x) = u^{(3)}_{,x}(x,h) - u^{(1)}_{,x}(x,h), \quad 0 < x < \infty, \tag{2.27b}$$

$$g_3(x) = v^{(1)}_{,x}(x,h) - v^{(2)}_{,x}(x,h), \quad 0 < x < \infty, \tag{2.27c}$$

$$g_4(x) = u^{(1)}_{,x}(x,h) - u^{(2)}_{,x}(x,h), \quad 0 < x < \infty, \tag{2.27d}$$

which satisfies the conditions

$$g_j(x) = 0, \qquad j = 1,2,\ x < e-b, x > e+b, \tag{2.28a}$$

$$g_j(x) = 0, \qquad j = 3,4,\ x > a, \tag{2.28b}$$

$$\int_{e-b}^{e+b} g_j(x)dx = 0, \qquad j = 1,\ 2, \tag{2.28c}$$

$$\int_{0}^{a} g_j(x)dx = 0, \qquad j = 3,\ 4. \tag{2.28d}$$

By the application of standard inverse Fourier transformation in density functions (2.27a)-(2.27d) and employing the boundary conditions on thermal stresses given in (2.20d)-(2.20e) and using the expressions given in (2.16a)-(2.16f), we obtain the expressions of the stress components as

$$\begin{bmatrix} \sigma^{(1)}_{yy}(x,h) \\ \sigma^{(1)}_{yy}(x,0) \end{bmatrix} = \int_{e-b}^{e+b} \begin{bmatrix} M_1 & M_2 \\ M_3 & M_4 \end{bmatrix} \begin{bmatrix} g_1(r) \\ g_2(r) \end{bmatrix} dr + \int_0^a \begin{bmatrix} M_3 & -M_4 \\ M_1 & M_2 \end{bmatrix} \begin{bmatrix} g_3(r) \\ g_4(r) \end{bmatrix} dr$$
$$+ \int_{e-b}^{e+b} \begin{bmatrix} N_1 \\ N_2 \end{bmatrix} \Big[f_1(r) \Big] dr + \int_0^a \begin{bmatrix} -N_2 \\ N_1 \end{bmatrix} \Big[f_2(r) \Big] dr, \quad 0 < x < \infty, \tag{2.29a}$$

$$\begin{bmatrix} \tau^{(1)}_{xy}(x,h) \\ \tau^{(1)}_{xy}(x,0) \end{bmatrix} = \int_{e-b}^{e+b} \begin{bmatrix} M_5 & M_6 \\ M_7 & M_8 \end{bmatrix} \begin{bmatrix} g_1(r) \\ g_2(r) \end{bmatrix} dr + \int_0^a \begin{bmatrix} -M_7 & M_8 \\ M_5 & M_6 \end{bmatrix} \begin{bmatrix} g_3(r) \\ g_4(r) \end{bmatrix} dr$$
$$+ \int_{e-b}^{e+b} \begin{bmatrix} N_3 \\ N_4 \end{bmatrix} \Big[f_1(r) \Big] dr + \int_0^a \begin{bmatrix} N_4 \\ N_3 \end{bmatrix} \Big[f_2(r) \Big] dr, \qquad 0 < x < \infty, \tag{2.29b}$$

where $M_i = M_i(x,r),\ i = 1(1)8$ are isothermal kernel functions and $N_j = N_j(x,r),\ j = 1(1)4$ are non-isothermal kernels given in the Appendix.

Identities (2.26a)-(2.26c) yield the Cauchy integral equations of the first kind for heat conduction problems and thermal stresses.

2.4 Integral Equations

The Cauchy singularity $1/(r-x)$ is associated with the cracks in the infinite orthotropic plane. The equations (2.24a)-(2.24b) can further be simplified into the integral equations as

$$\int_{e-b}^{e+b} k_1(x,r)f_1(r)dr + \int_0^a k_2(x,r)f_2(r)dr = \frac{-2\pi q_0}{\sqrt{k_x k_y}}, \qquad e-b < x < e+b, \tag{2.30a}$$

$$\int_{e-b}^{e+b} k_2(x,r)f_1(r)dr + \int_0^a k_1(x,r)f_2(r)dr = \frac{-2\pi q_0}{\sqrt{k_x k_y}}, \qquad 0 < x < a. \tag{2.30b}$$

The expressions (2.29a)-(2.29b) generate the following set of quadruple integral equations, including the forcing terms depending on temperature as

$$\begin{aligned} &\wedge_1 \int_{e-b}^{e+b} k_1(x,r)g_1(r)dr + \int_0^a (m_1 k_3(x,r) + m_2 k_4(x,r))g_3(r)dr \\ &\quad + m_3 \int_0^a k_5(x,r)g_4(r)dr = -l_1\pi + \int_0^a p_1(x,r)f_2(r)dr, \quad e-b < x < e+b, \end{aligned} \tag{2.31a}$$

$$\begin{aligned} &\int_{e-b}^{e+b} (m_1 k_3(x,r) + m_2 k_4(x,r))g_1(r)dr - m_3 \int_{e-b}^{e+b} k_5(x,r)g_2(r)dr \\ &\quad + \wedge_1 \int_0^a k_1(x,r)g_3(r)dr = -l_2\pi + \int_{e_b}^{e+b} -p_1(x,r)f_1(r)dr, \quad 0 < x < a, \end{aligned} \tag{2.31b}$$

$$-\wedge_2 \int_{e-b}^{e+b} k_1'(x,r)g_2(r)dr + m_4 \int_0^a k_5'(x,r)g_3(r)dr + \int_0^a (-m_5 k_3'(x,r) - m_6 k_4'(x,r))$$
$$g_4(r)dr = -n_5 \int_{e-b}^{e+b} h(x,r)f_1(r)dr - \int_0^a p_2(x,r)f_2(r)dr,\ |x-e| < b, \quad (2.31c)$$
$$-m_4 \int_{e-b}^{e+b} k_5'(x,r)g_1(r)dr + \int_{e-b}^{e+b} (-m_5 k_3'(x,r) - m_6 k_4'(x,r))g_2(r)dr - \wedge_2$$
$$\int_0^a k_1'(x,r)g_4(r)dr = -\int_{e-b}^{e+b} p_2(x,r)f_1(r)dr - n_5 \int_0^a h(x,r)f_2(r)dr,\ x < a, \quad (2.31d)$$

where the kernels containing the singularity term are expressed as

$$k_1(x,r) = \frac{1}{r+x} + \frac{1}{r-x}, \quad (2.32a)$$
$$k_1'(x,r) = \frac{1}{r+x} - \frac{1}{r-x}, \quad (2.32b)$$
$$k_2(x,r) = \frac{r+x}{(kh)^2+(r+x)^2} + \frac{r-x}{(kh)^2+(r-x)^2}, \quad (2.32c)$$
$$k_j(x,r) = \frac{r+x}{(\lambda_{j-2}h)^2+(r+x)^2} + \frac{r-x}{(\lambda_{j-2}h)^2+(r-x)^2}, j = 3,4, \quad (2.32d)$$
$$k_j'(x,r) = \frac{r+x}{(\lambda_{j-2}h)^2+(r+x)^2} - \frac{r-x}{(\lambda_{j-2}h)^2+(r-x)^2}, j = 3,4, \quad (2.32e)$$
$$k_5(x,r) = \frac{\lambda_1 h}{(\lambda_1 h)^2+(r+x)^2} - \frac{\lambda_2 h}{(\lambda_2 h)^2+(r+x)^2} + \frac{\lambda_1 h}{(\lambda_1 h)^2+(r-x)^2} - \frac{\lambda_2 h}{(\lambda_2 h)^2+(r-x)^2}, \quad (2.32f)$$
$$k_5'(x,r) = \frac{\lambda_1 h}{(\lambda_1 h)^2+(r+x)^2} - \frac{\lambda_2 h}{(\lambda_2 h)^2+(r+x)^2} - \frac{\lambda_1 h}{(\lambda_1 h)^2+(r-x)^2} + \frac{\lambda_2 h}{(\lambda_2 h)^2+(r-x)^2}, \quad (2.32g)$$

and the kernels $p_j(x,r), j = 1,2$ in the non isothermal forcing terms are defined by

$$p_1(x,r) = n_1 \left(\tan^{-1}\frac{r+x}{\lambda_1 h} + \tan^{-1}\frac{r-x}{\lambda_1 h}\right) + n_2 \left(\tan^{-1}\frac{r+x}{\lambda_2 h} + \tan^{-1}\frac{r-x}{\lambda_2 h}\right)$$
$$+ \sigma_T \left(\tan^{-1}\frac{r+x}{kh} + \tan^{-1}\frac{r-x}{kh}\right), \quad (2.33a)$$
$$p_2(x,r) = n_3 \int_0^\infty \frac{1}{s} e^{-s\lambda_1 h} \sin(sr)\sin(sx)ds + n_4 \int_0^\infty \frac{1}{s} e^{-s\lambda_2 h} \sin(sr)\sin(sx)ds$$

$$+ \tau_T \int_0^\infty \frac{1}{s} e^{-skh} \sin(sr) \sin(sx) ds, \tag{2.33b}$$

$$h(x,r) = \int_0^\infty \frac{1}{s} \sin(sr) \sin(sx) ds, \tag{2.33c}$$

$p_2(x,r)$ and $h(x,r)$ are evaluated numerically in the further calculations. The expressions of $n_j, j = 1(1)5$ and σ_T and τ_T and $\wedge_j, j = 1,2$ and $m_j, j = 1(1)6$ are given in equations (A.4) in Appendix.

2.5 Numerical Method

A numerical method to find the solutions of two groups of singular integral equations of the first kind given in equations (2.30a)-(2.30b) and (2.31a)-(2.31d) is discussed in the present section. The equations are formulated from the governing equations of motion and mixed boundary conditions applied to heat conduction and thermal stress fields. The distinguishing feature of the obtained integral equations is the presence of Cauchy kernel. These can be regularized by the method given by Mushkelisvili [71]. The chapter discusses the numerical solutions with the help of Chebyshev polynomial functions on the finite interval $[-1, 1]$.

Following the methodology explained in Chapter 1, 1.7.1.1, we proceed to solve the obtained integral equations. The auxiliary functions defined previously are expressed in the form of bounded functions $\phi(r), \psi(r)$ defined on the normalized intervals given as

$$(x,r) = (b\xi + e, b\eta + e), \tag{2.34a}$$

$$(x,r) = (a(\xi+1)/2, a(\eta+1)/2), \qquad -1 < (\xi,\eta) < 1. \tag{2.34b}$$

Considering the infinite series with Chebyshev polynomial of the first kind as

$$f_i(\eta) = \frac{1}{\sqrt{(1-\eta^2)}} \sum_{n=0}^{\infty} c_{in} T_n(\eta), i = 1, 2, \tag{2.35}$$

$$g_j(\eta) = \frac{1}{\sqrt{(1-\eta^2)}} \sum_{n=0}^{\infty} d_{jn} T_n(\eta), j = 1(1)4, \tag{2.36}$$

where c_{in}, $i = 1, 2$ and d_{jn}, $j = 1(1)4$ are unknown coefficients, and using the orthogonality condition and truncating the series at $n = N$, we are able to regularize the integral equations to obtain the expressions for SIFs and heat fluxes at the tips of the cracks [72].

Applying the standard definition of SIFs at the inner and outer parts of the tips of the cracks, we get

$$K_{I(a)} = \lim_{x \to a+} \sqrt{2(x-a)} \sigma_{yy}^{(1)}(x, 0) = - \wedge_1 \frac{\sqrt{a}}{2} \sum_{n=1}^{N} d_{3n}, \tag{2.37a}$$

$$K_{I(e-b)} = \lim_{x \to (e-b)-} \sqrt{2(e-b-x)} \sigma_{yy}^{(1)}(x, h) = \wedge_1 \frac{\sqrt{b}}{2} \sum_{n=1}^{N} (-1)^n d_{1n}, \tag{2.37b}$$

$$K_{I(e+b)} = \lim_{x \to (e+b)+} \sqrt{2(x-e-b)} \sigma_{yy}^{(1)}(x, h) = - \wedge_1 \frac{\sqrt{b}}{2} \sum_{n=1}^{N} d_{1n}. \tag{2.37c}$$

It should be noted that K_I's denote the mode I SIFs, and the subscripts (a), $(e-b)$, $(e+b)$ specify the considered cracks' tips.

2.6 Results and Discussion

In this section, the SIFs at the tips of the central crack and the offset parallel cracks and their interaction for different lengths and heights of the cracks are found for different cases and displayed graphically. Numerical calculations are carried out for the FRC material with carbon-based fiber(T300 Graphite) and matrix(epoxy)

whose material constants are given in Table 2.1 [73]. Here, the subscripts f_1, f_2, and m are for the longitudinal, transversal direction of the fibre phase and isotropic matrix phases, respectively. V_F is the fiber volume fraction depending on which the composite micro-mechanics equations are employed to calculate material constants. During numerical computations, N is increased until the repetition of three significant digits in the calculation of SIFs. The normalizing factor for crack tip SIF is chosen as $K_0 = (n_5 q_0 a^{3/2})/(2\sqrt{k_x k_y})$ and $l_1 = l_2 = 10$ MPa. For simplicity, $K_{I(a)} = K_{I(a)}/K_0$ is taken. Figure 2.2 indicates the effect of offset parallel crack on $K_{I(a)}$. For a fixed height $a/h = 0.5$, length of central crack $a/(e+b) = 0.5$ and varying values of offset parallel crack's length viz., $(e-b)/(e+b)$ from 0.55 to 0.9, it is observed from Figure 2.2 that as the length of outer crack increases, mode I SIF at the crack tip $x = a$ decreases. In other words, as the offset crack moves away from the central crack, the SIF at the tip of the central crack decreases.

Therefore, from the above discussion, it can be concluded that as the distance between the central and offset parallel crack decreases, SIFs at the crack tip increase. The effects of height on normalized mode I SIFs are demonstrated through Figure 2.4 and Figure 2.5. For fixed $a/(e+b) = 0.5$, $(e-b)/(e+b) = 0.6$ and different values of a/h viz., 0.5 to 2.5, Figure 2.4 shows that as the height increases mode I SIF at the central crack tip decreases.

Keeping the length of parallel offset crack fixed $(e-b)/(e+b) = 0.6$ and varying $a/(e+b)$ from 0.2 to 0.55, it can be noted from the Figure 2.3 that the values of normalized mode I SIFs at the crack tips $(e-b)$ and $(e+b)$ increases.
Similar behaviour is observed for the normalized mode I SIFs at the crack tips $(e-b)$ and $(e+b)$. Thus, it can be said that as the height increases, the SIFs at the crack

TABLE 2.1: Values of material constants for the considered orthotropic material.

k_{f_1}	84 W.(m.K)$^{-1}$	k_x	42.1 W.(m.K)$^{-1}$
k_{f_2}	84 W.(m.K)$^{-1}$	k_y	0.466 W.(m.K)$^{-1}$
k_m	84 W.(m.K)$^{-1}$	ν_m	0.35
E_{f_1}	$220.6 \times 10^{+6}$ kPa	E_x	$112 \times 10^{+6}$ kPa
E_{f_2}	$13.8 \times 10^{+6}$ kPa	E_y	$7.35 \times 10^{+6}$ kPa
E_m	$3.45 \times 10^{+6}$ kPa	G_{xy}	$3.24 \times 10^{+6}$ kPa
G_{f_1}	$8.9 \times 10^{+6}$ kPa	ν_{f_1}	0.2
G_{f_2}	$4.8 \times 10^{+6}$ kPa	ν_{f_2}	0.25
G_m	$1.28 \times 10^{+6}$ kPa	ν_{xy}	0.275
α_{f_1}	-0.98×10^{-6} K^{-1}	α_x	0.025×10^{-6} K^{-1}
α_{f_2}	10×10^{-6} K^{-1}	α_y	32.4×10^{-6} K^{-1}
α_m	64.3×10^{-6} K^{-1}	V_F	0.5

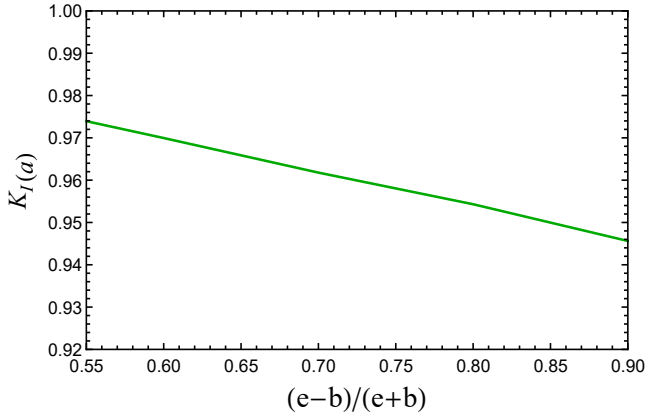

FIGURE 2.2: Variation of normalized mode I SIF at the crack tip a for different values of $(e-b)/(e+b)$.

tip decrease.

2.7 Conclusion

A problem of three thermally insulated cracks in an orthotropic plane with a particular case of FRC material has been solved. The considered infinite orthotropic plane is subjected to thermo-mechanical loading. The chapter specifically addresses the interaction between cracks, considering their various length-to-height ratios. The

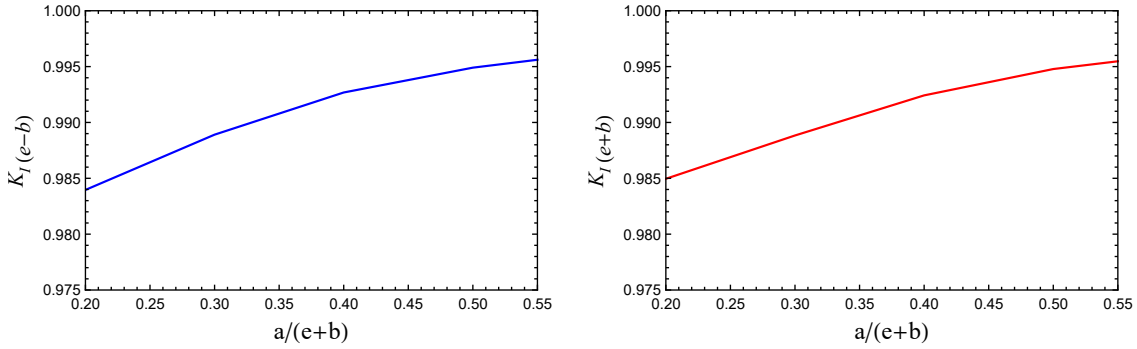

FIGURE 2.3: Variations of (a) $K_{I(e-b)}$ and (b) $K_{I(e+b)}$ for different values of $a/(e+b)$.

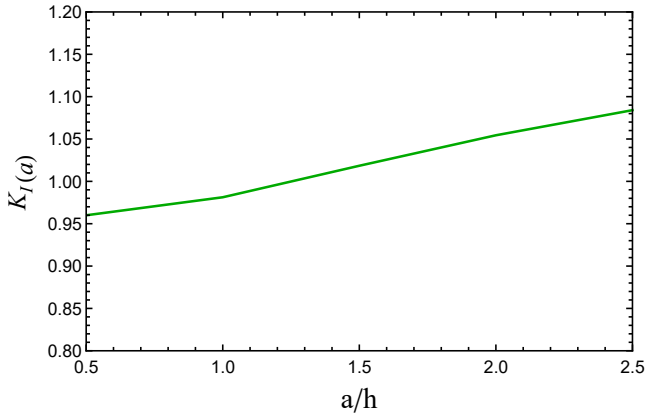

FIGURE 2.4: Plot of normalized mode I SIF at the crack tip a for different values of a/h.

main aim of the chapter is to find the expressions of mode-I SIFs at the vicinity of each crack's tip. The most important part of the study is the presentation of increasing and decreasing tendencies of the propagation of offset cracks due to variations in the lengths and distance of the cracks through the pictorial presentations of SIFs. With the help of the first kind of Chebyshev polynomial, the expansion collocation method was employed to carry out the numerical computations. The scope of the study can be extended to the interaction of the cracks in a sandwiched orthotropic strip with the offset cracks at the interfaces of dissimilar planes under thermo-mechanical loading. The perfectly insulated cracks can be replaced with a thermally permeable crack model, increasing the scope of the study. These types

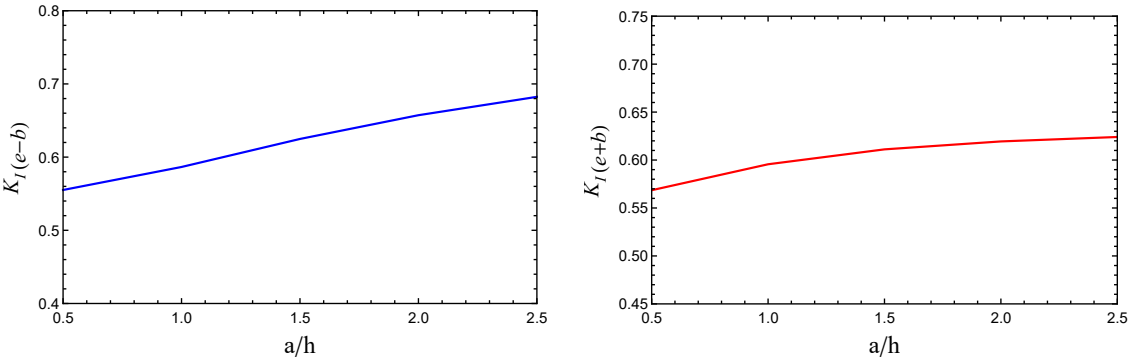

FIGURE 2.5: Plots of (a) $K_{I(e-b)}$ and (b) $K_{I(e+b)}$ for different values of a/h.

of problems have been considered in the subsequent chapters, with cracks under mechanical loadings present in the dissimilar orthotropic medium.

****